On the usefulness of electron propagator methods for a reliable computation of experimental observables

Lorenzo Paoloni[1]

[1]Dipartimento di Fisica e Astronomia, Università degli Studi di Padova (Italy)

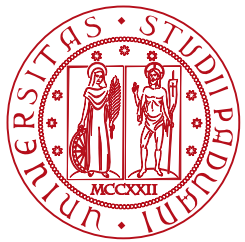

Università degli Studi di Padova

Overview of this presentation

- Electron propagator methods
- Computational simulation of vibrationally resolved ultraviolet photoelectron spectra (UPS)
  - Description of the computational protocol
  - Application to 6 organic molecules*
- From gas phase to solutions: missing part
- Acknowledgements

*Published in:
L. Paoloni, M. Fusé, A. Baiardi, V. Barone, *J. Chem. Theory Comput.*, **2020**, 16, 5218-5226.

Electron propagator theory: the spectral representation

- A unified treatment of ionization processes
  - Electron detachment: $A \longrightarrow A^+ + e^-$
  - Electron attachment: $A + e^- \longrightarrow A^-$
- A feasible computational approach to systematically improve estimates based on Koopmans' theorem

See:
J. Linderberg, Y. Öhrn, *Propagators in Quantum Chemistry*, **2004**;
J. V. Ortiz, *WIREs Computational Molecular Science*, **2013**, 3, 123 - 142.

Electron propagator theory: the spectral representation

- A unified treatment of ionization processes
  - Electron detachment: $A \longrightarrow A^+ + e^-$
  - Electron attachment: $A + e^- \longrightarrow A^-$
- A feasible computational approach to systematically improve estimates based on Koopmans' theorem

Propagators (or double time green's functions) are often studied in terms of their spectral representation

$$G_{pq}(E) = \langle\langle a_p^\dagger ; a_q \rangle\rangle_E =$$

$$\lim_{\eta \to +0} \left[\sum_n \frac{\left\langle \phi_0^{N_{el}} \middle| a_p^\dagger \middle| \phi_n^{N_{el}-1} \right\rangle \left\langle \phi_n^{N_{el}-1} \middle| a_q \middle| \phi_0^{N_{el}} \right\rangle}{E + E_n^{N_{el}-1} - E_0^{N_{el}} - i\eta} + \sum_m \frac{\left\langle \phi_0^{N_{el}} \middle| a_q \middle| \phi_m^{N_{el}+1} \right\rangle \left\langle \phi_m^{N_{el}+1} \middle| a_p^\dagger \middle| \phi_0^{N_{el}} \right\rangle}{E - E_m^{N_{el}+1} + E_0^{N_{el}} + i\eta} \right].$$

- $G_{pq}(E)$ is an element of the matrix $\mathbf{G}(E)$

$p, q \equiv$ spin-orbital indices

$a_p^\dagger \equiv$ destruction operator

$a_q \equiv$ creation operator

$\phi_0^{N_{el}} \equiv$ electronic ground state of the N_{el}-electron system

$\phi_n^{N_{el}-1} \equiv$ electronic state n of the $(N_{el}-1)$-electron system

$\phi_m^{N_{el}+1} \equiv$ electronic state m of the $(N_{el}+1)$-electron system

---

See:
J. Linderberg, Y. Öhrn, *Propagators in Quantum Chemistry*, **2004**;
J. V. Ortiz, *WIREs Computational Molecular Science*, **2013**, 3, 123 - 142.

Electron propagator theory: the spectral representation

- A unified treatment of ionization processes
  - Electron detachment: $A \longrightarrow A^+ + e^-$
  - Electron attachment: $A + e^- \longrightarrow A^-$
- A feasible computational approach to systematically improve estimates based on Koopmans' theorem

Propagators (or double time green's functions) are often studied in terms of their spectral representation

$$G_{pq}(E) = \langle\langle a_p^\dagger ; a_q \rangle\rangle_E =$$

$$\lim_{\eta \to +0} \left[\sum_n \frac{\left\langle \phi_0^{N_{el}} \middle| a_p^\dagger \middle| \phi_n^{N_{el}-1} \right\rangle \left\langle \phi_n^{N_{el}-1} \middle| a_q \middle| \phi_0^{N_{el}} \right\rangle}{E + E_n^{N_{el}-1} - E_0^{N_{el}} - i\eta} + \sum_m \frac{\left\langle \phi_0^{N_{el}} \middle| a_q \middle| \phi_m^{N_{el}+1} \right\rangle \left\langle \phi_m^{N_{el}+1} \middle| a_p^\dagger \middle| \phi_0^{N_{el}} \right\rangle}{E - E_m^{N_{el}+1} + E_0^{N_{el}} + i\eta} \right].$$

$p, q \equiv$ spin-orbital indices

$a_p^\dagger \equiv$ destruction operator

$a_q \equiv$ creation operator

$\phi_0^{N_{el}} \equiv$ electronic ground state of the N_{el}-electron system

$\phi_n^{N_{el}-1} \equiv$ electronic state n of the $(N_{el}-1)$-electron system

$\phi_m^{N_{el}+1} \equiv$ electronic state m of the $(N_{el}+1)$-electron system

- $G_{pq}(E)$ is an element of the matrix $\mathbf{G}(E)$

Poles correspond to $E = E_n^{N_{el}+1} - E_0^{N_{el}}$ (electron affinities) and $E = E_0^{N_{el}} - E_n^{N_{el}-1}$ (ionization potentials)

See:
J. Linderberg, Y. Öhrn, *Propagators in Quantum Chemistry*, **2004**;
J. V. Ortiz, *WIREs Computational Molecular Science*, **2013**, 3, 123 - 142.

Electron propagator methods: the self-energy

- the inverse of the matrix $\mathbf{G}(E)$ can be written as follows:

$$\mathbf{G}^{-1}(E) = E\mathbf{I} - \mathbf{F}^{gen} - \boldsymbol{\sigma}(E)$$

  - $\mathbf{F}^{gen}$ is a generalized Fock matrix ($\mathbf{F}^{gen} = \mathbf{F} + \boldsymbol{\Sigma}(\infty)$)
  - $\boldsymbol{\sigma}(E)$ is the (energy-dependent) self-energy term
- $det\ \mathbf{G}(E)$ diverges when $det\ \mathbf{G}^{-1}(E) = 0$

*For example:
outer valence Green's function (OVGF), partial third-order (P3) or diagonal second-order (D2) approximations

Electron propagator methods: the self-energy

- the inverse of the matrix $\mathbf{G}(E)$ can be written as follows:

$$\mathbf{G}^{-1}(E) = E\mathbf{I} - \mathbf{F}^{gen} - \boldsymbol{\sigma}(E)$$

  - $\mathbf{F}^{gen}$ is a generalized Fock matrix ($\mathbf{F}^{gen} = \mathbf{F} + \boldsymbol{\Sigma}(\infty)$)
  - $\boldsymbol{\sigma}(E)$ is the (energy-dependent) self-energy term
- $det\ \mathbf{G}(E)$ diverges when $det\ \mathbf{G}^{-1}(E) = 0$

i.e. when the energy E is equal to a pole (E_{pole}):

$$[\mathbf{F}^{gen} + \boldsymbol{\sigma}(E_{pole})]\mathbf{C}(E_{pole}) = E_{pole}\mathbf{C}(E_{pole})$$

*For example:
outer valence Green's function (OVGF), partial third-order (P3) or diagonal second-order (D2) approximations

Electron propagator methods: the self-energy

- the inverse of the matrix $\mathbf{G}(E)$ can be written as follows:
$$\mathbf{G}^{-1}(E) = E\mathbf{I} - \mathbf{F}^{gen} - \boldsymbol{\sigma}(E)$$
  - $\mathbf{F}^{gen}$ is a generalized Fock matrix ($\mathbf{F}^{gen} = \mathbf{F} + \boldsymbol{\Sigma}(\infty)$)
  - $\boldsymbol{\sigma}(E)$ is the (energy-dependent) self-energy term
- $det\ \mathbf{G}(E)$ diverges when $det\ \mathbf{G}^{-1}(E) = 0$

i.e. when the energy E is equal to a pole (E_{pole}):

$$[\mathbf{F}^{gen} + \boldsymbol{\sigma}(E_{pole})]\mathbf{C}(E_{pole}) = E_{pole}\mathbf{C}(E_{pole})$$

The method depends on the choice of $\boldsymbol{\Sigma}(E) = \boldsymbol{\Sigma}(\infty) + \boldsymbol{\sigma}(E)$

- $\boldsymbol{\Sigma}(E) = 0$: Hartee-Fock approximation
- $\Sigma_{pq}(E) = 0$ if $p \neq q$: diagonal approximations*
- Otherwise: non - diagonal approximations

Diagonal approximations are often a good compromise between accuracy and computational cost

---

*For example:
outer valence Green's function (OVGF), partial third-order (P3) or diagonal second-order (D2) approximations

Computational simulation of vibrationally resolved ultraviolet photoelectron spectra

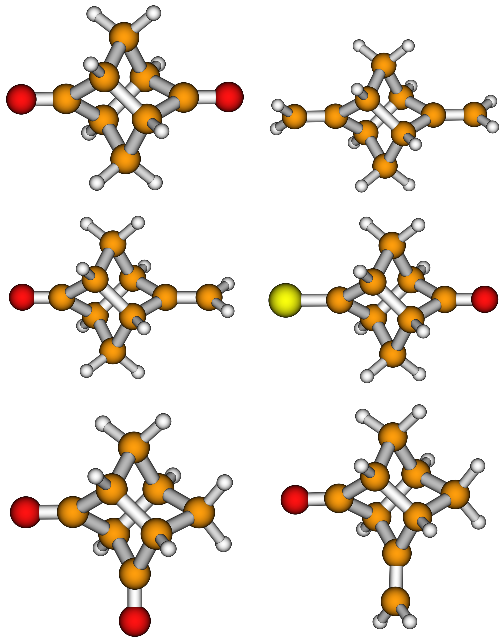

Structural features

- Rigid σ-scaffold
- two π-bonds (separated by the central σ-scaffold)

- Electronic and nuclear pieces of information are intertwined in the experimental data
- Validation of a computational approach based on a composite scheme:

  electron propagator theory

  $+$

  Franck-Condon and vertical gradient approximations
- The composite scheme is expected to be effective for:
  - Semi-rigid molecular systems
  - Systems where the effects of LAMs on the experimental ultraviolet photoelectron spectrum is negligible

Computational strategy

Vertical gradient approximation

Duschinsky transformation: $\overline{\mathbf{Q}} = \mathbf{J}\overline{\overline{\mathbf{Q}}} + \mathbf{K}$

- Assumptions:
  - $\mathbf{J} = \mathbf{I}$
  - $\mathbf{K} = f(\overline{\overline{\mathbf{g}}})$

Franck-Condon approximation

$$\left\langle \overline{\chi_i} \middle| \boldsymbol{\mathcal{T}}^e_{IF} \middle| \overline{\overline{\chi_f}} \right\rangle \approx \boldsymbol{\mathcal{T}}^e_{IF}(\overline{\mathbf{Q}}_{eq}) \left\langle \overline{\chi_i} \middle| \overline{\overline{\chi_f}} \right\rangle$$

Approximation of the electron propagator matrix

- diagonal approaches:
  - Outer Valence Green's Functions (OVGF) method
- non-diagonal approaches:
  - Non-diagonal renormalized second-order (NR2) approximation
- basis set: maug-cc-pVTZ

Computational protocol

- 1. geometry optimization and calculation of harmonic frequencies at B3LYP/maug-cc-pVTZ level of theory
- 2. Calculation of vertical ionization energies (VIEs) at NR2/maug-cc-pVTZ level of theory
- 3. Calculation of $\overline{\overline{\mathbf{g}}}_x$ through numerical differentiation† of VIEs calculated at OVGF/maug-cc-pVTZ level of theory
- 4. Calculation of relative intensities through a time-independent (TI) approach

†Mathematical formulations suitable for the analytical differentiation are available in literature; see:
J. V. Ortiz, *J. Chem. Phys.*, **2000**, 112, 56 - 68.

The case of stella-2,6-dione

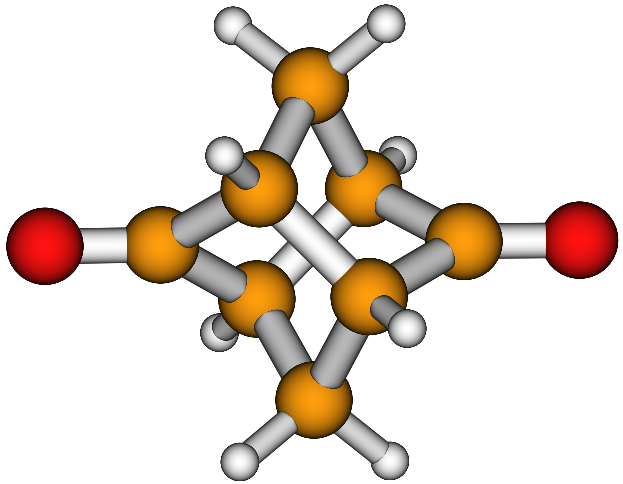

Experimental data reported in:
R. Gleiter, H. Lange, O. Borzyk, *J. Am. Chem. Soc.*, **1996**, 118, 4889 - 4895.

Computational results published in:
L. Paoloni, M. Fusé, A. Baiardi, V. Barone, *J. Chem. Theory Comput.*, **2020**, 16, 5218-5226.

The case of stella-2,6-dione

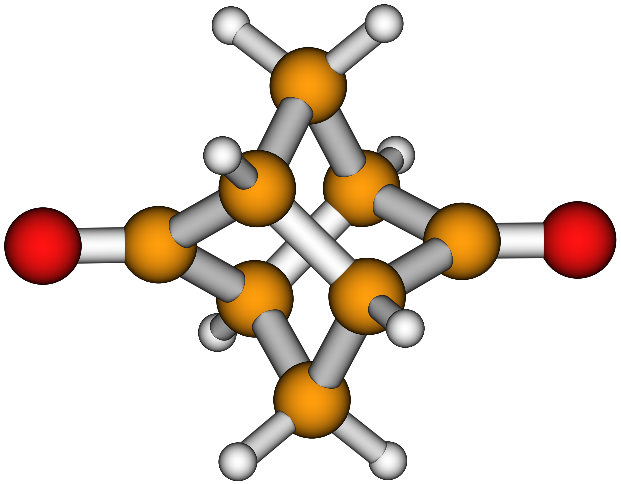

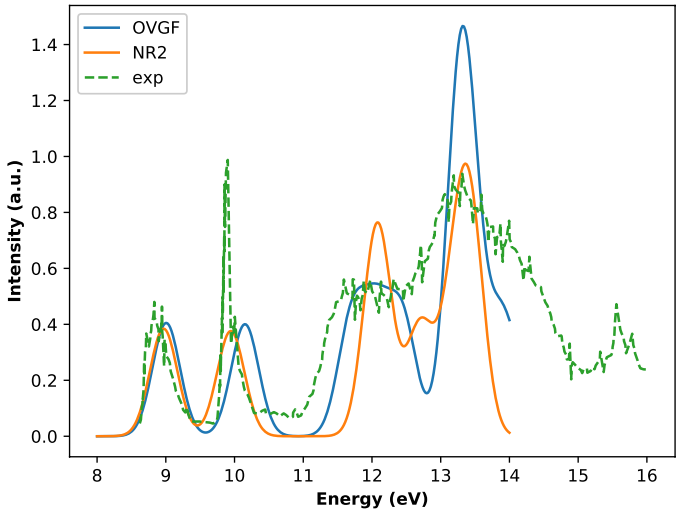

Comparison between calculated and experimental spectra

Experimental data reported in:
R. Gleiter, H. Lange, O. Borzyk, *J. Am. Chem. Soc.*, **1996**, 118, 4889 - 4895.

Computational results published in:
L. Paoloni, M. Fusé, A. Baiardi, V. Barone, *J. Chem. Theory Comput.*, **2020**, 16, 5218-5226.

The case of stella-2,6-dione

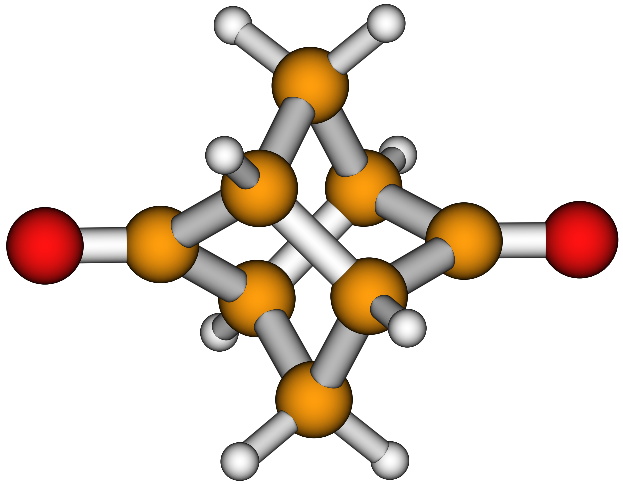

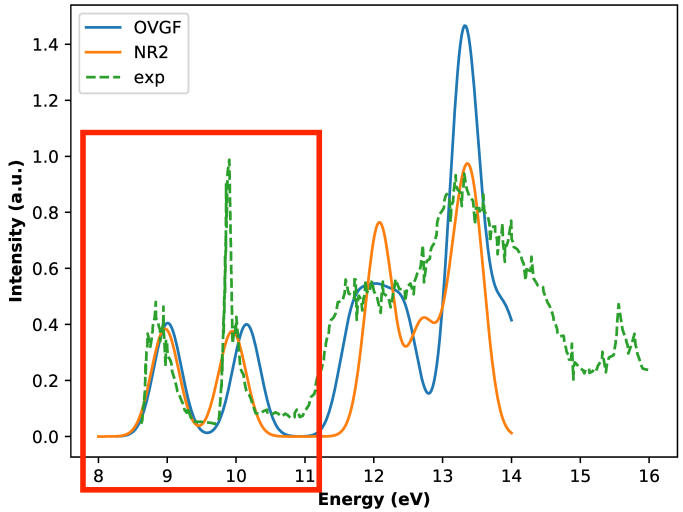

Comparison between calculated and experimental spectra

- Similar results with diagonal and non-diagonal approximations in the outer valence region

---

Experimental data reported in:
R. Gleiter, H. Lange, O. Borzyk, *J. Am. Chem. Soc.*, **1996**, 118, 4889 - 4895.

Computational results published in:
L. Paoloni, M. Fusé, A. Baiardi, V. Barone, *J. Chem. Theory Comput.*, **2020**, 16, 5218-5226.

The case of stella-2,6-dione

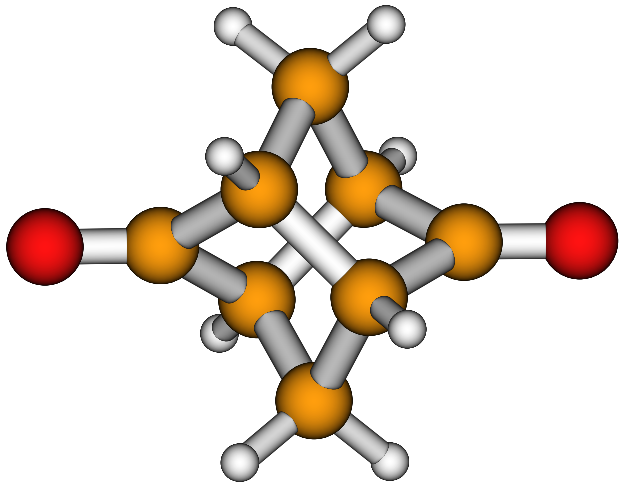

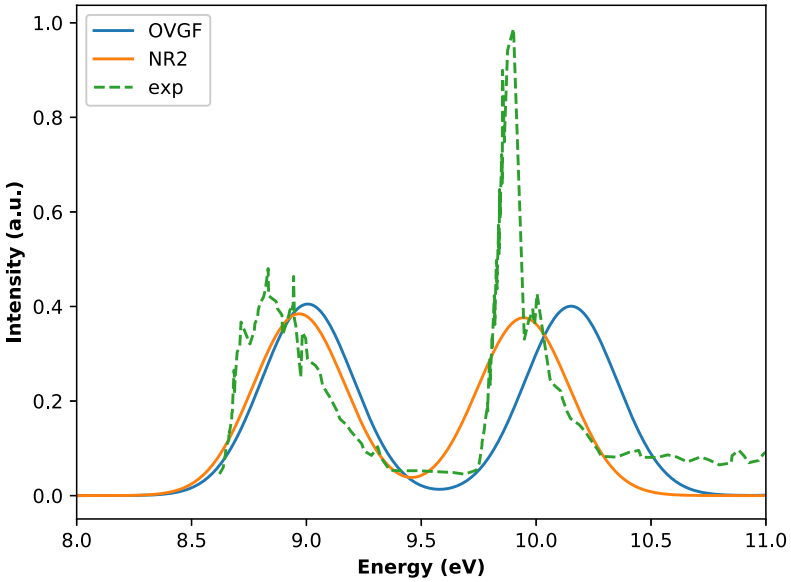

Comparison between calculated and experimental spectra

- Similar results with diagonal and non-diagonal approximations in the outer valence region

---

Experimental data reported in:
R. Gleiter, H. Lange, O. Borzyk, *J. Am. Chem. Soc.*, **1996**, 118, 4889 - 4895.

Computational results published in:
L. Paoloni, M. Fusé, A. Baiardi, V. Barone, *J. Chem. Theory Comput.*, **2020**, 16, 5218-5226.

The case of stella-2,6-dione

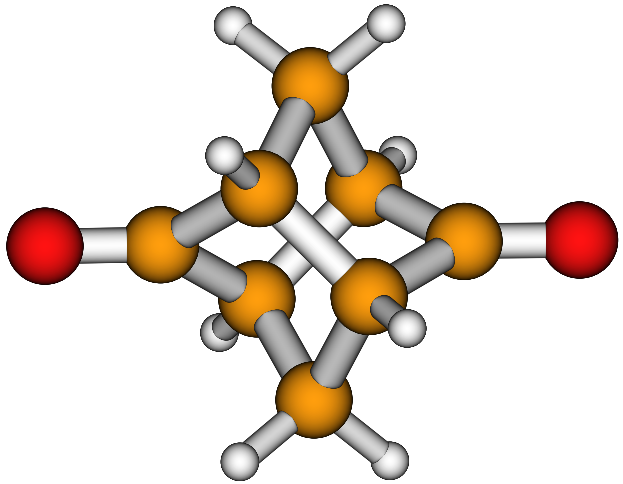

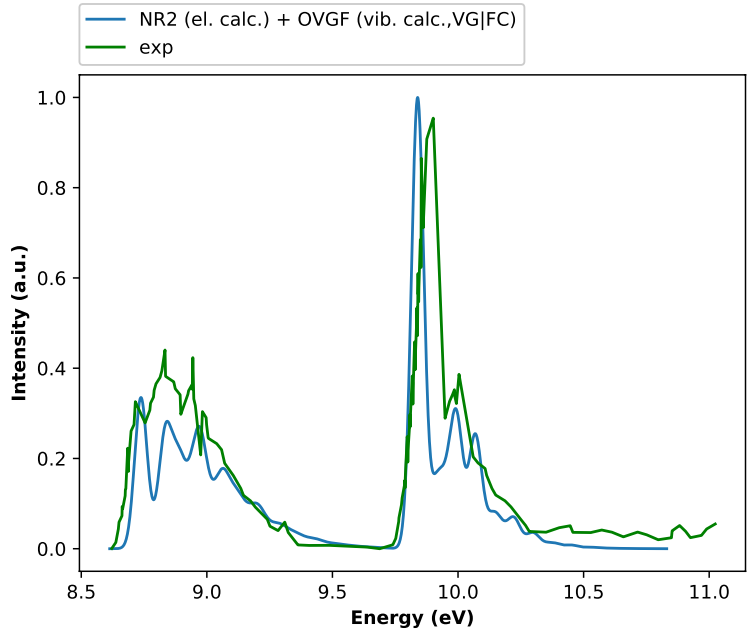

Comparison between calculated and experimental spectra

- Similar results with diagonal and non-diagonal approximations in the outer valence region
- Computation of band shapes $\longrightarrow$ The inclusion of vibronic signatures is pivotal

Experimental data reported in:
R. Gleiter, H. Lange, O. Borzyk, *J. Am. Chem. Soc.*, **1996**, 118, 4889 - 4895.

Computational results published in:
L. Paoloni, M. Fusé, A. Baiardi, V. Barone, *J. Chem. Theory Comput.*, **2020**, 16, 5218-5226.

Calculated and experimental spectra (1)

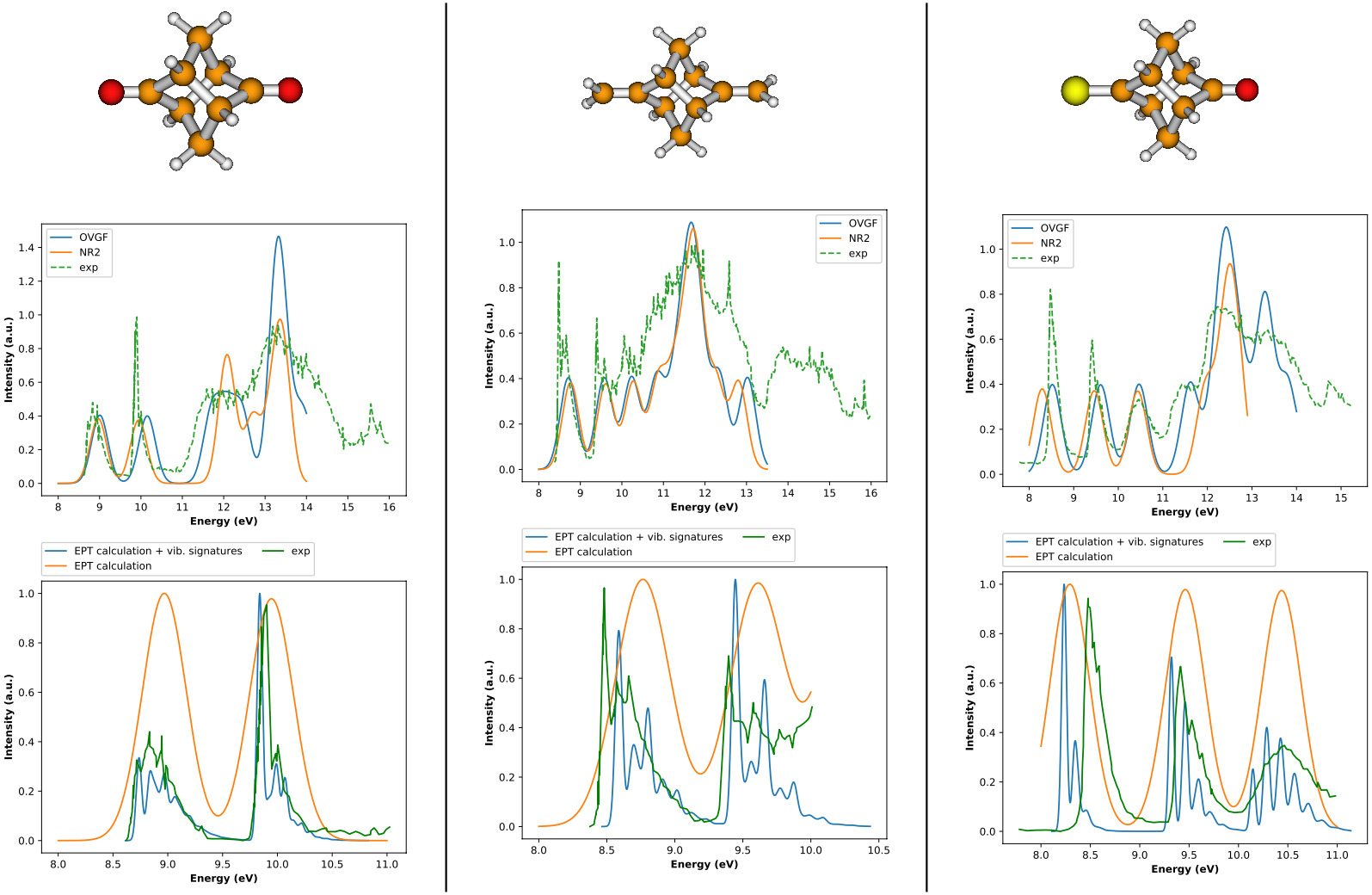

Experimental data reported in:
R. Gleiter, H. Lange, O. Borzyk, *J. Am. Chem. Soc.*, **1996**, 118, 4889 - 4895;
R. Gleiter, B. Gaa, C. Sigwart et al., *Eur. J. Chem.*, **1998**, 171-176.

Computational results published in:
L. Paoloni, M. Fusé, A. Baiardi, V. Barone, *J. Chem. Theory Comput.*, **2020**, 16, 5218-5226.

Calculated and experimental spectra (2)

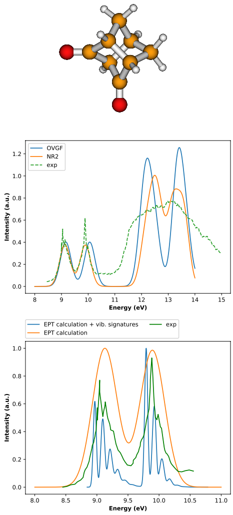

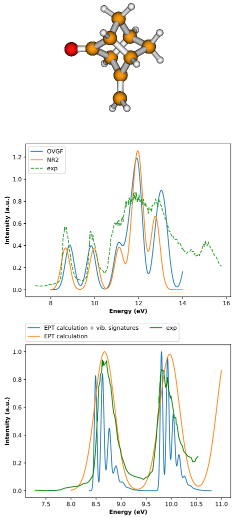

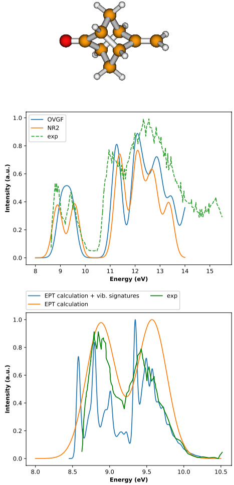

Experimental data reported in:
R. Gleiter, H. Lange, O. Borzyk, *J. Am. Chem. Soc.*, **1996**, 118, 4889 - 4895;
R. Gleiter, B. Gaa, C. Sigwart et al., *Eur. J. Chem.*, **1998**, 171-176.

Computational results published in:
L. Paoloni, M. Fusé, A. Baiardi, V. Barone, *J. Chem. Theory Comput.*, **2020**, 16, 5218-5226.

The case of stella-6-en-2-one

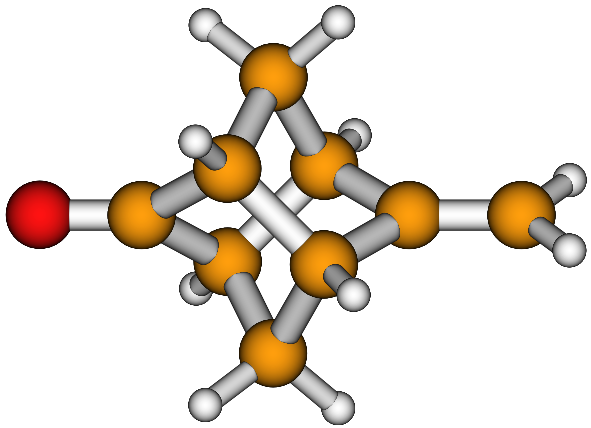

Experimental data reported in:
R. Gleiter, H. Lange, O. Borzyk, *J. Am. Chem. Soc.*, **1996**, 118, 4889 - 4895.

Computational results published in:
L. Paoloni, M. Fusé, A. Baiardi, V. Barone, *J. Chem. Theory Comput.*, **2020**, 16, 5218-5226.

The case of stella-6-en-2-one

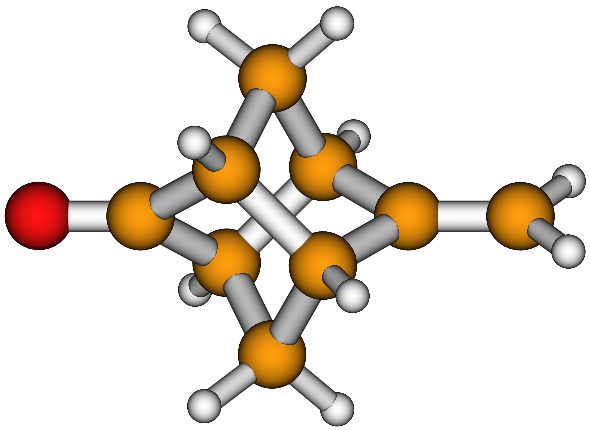

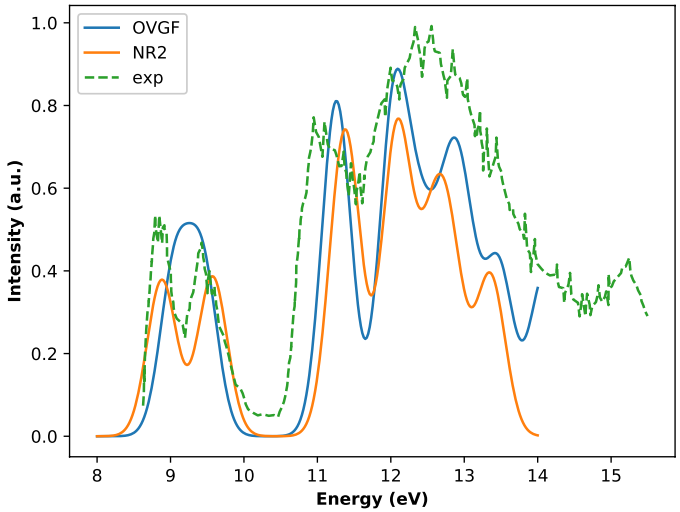

Comparison between calculated and experimental spectra

Experimental data reported in:
R. Gleiter, H. Lange, O. Borzyk, *J. Am. Chem. Soc.*, **1996**, 118, 4889 - 4895.

Computational results published in:
L. Paoloni, M. Fusé, A. Baiardi, V. Barone, *J. Chem. Theory Comput.*, **2020**, 16, 5218-5226.

The case of stella-6-en-2-one

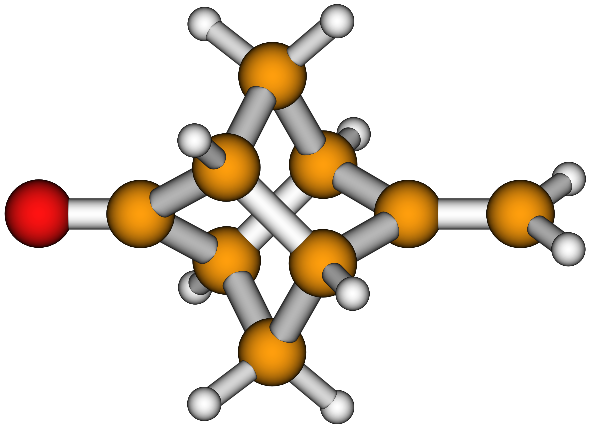

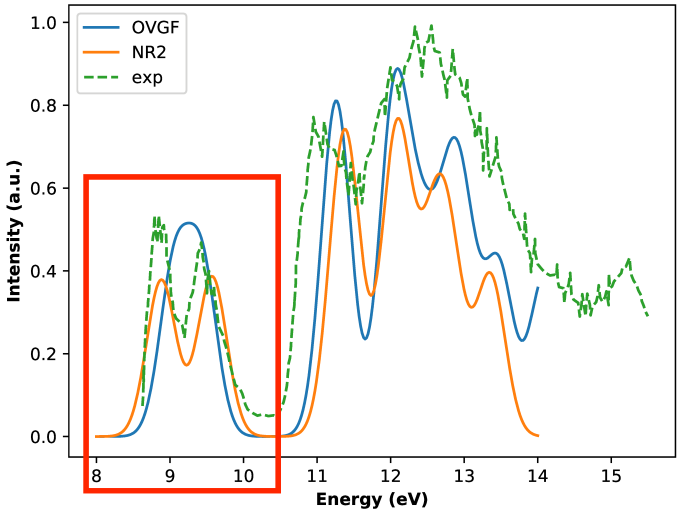

Comparison between calculated and experimental spectra

- Calculated VIEs at NR2 level are closer to experimental results in the outer valence region

---

Experimental data reported in:
R. Gleiter, H. Lange, O. Borzyk, *J. Am. Chem. Soc.*, **1996**, 118, 4889 - 4895.

Computational results published in:
L. Paoloni, M. Fusé, A. Baiardi, V. Barone, *J. Chem. Theory Comput.*, **2020**, 16, 5218-5226.

The case of stella-6-en-2-one

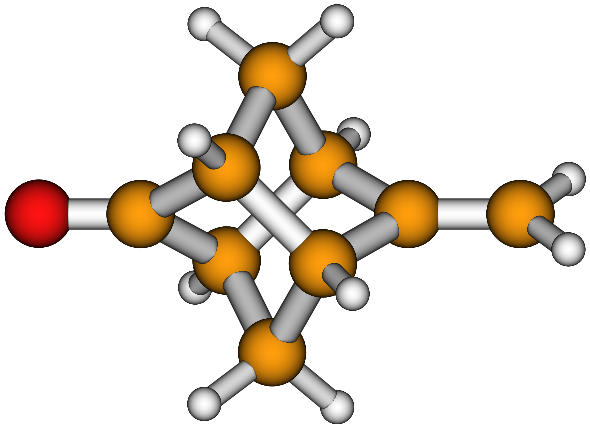

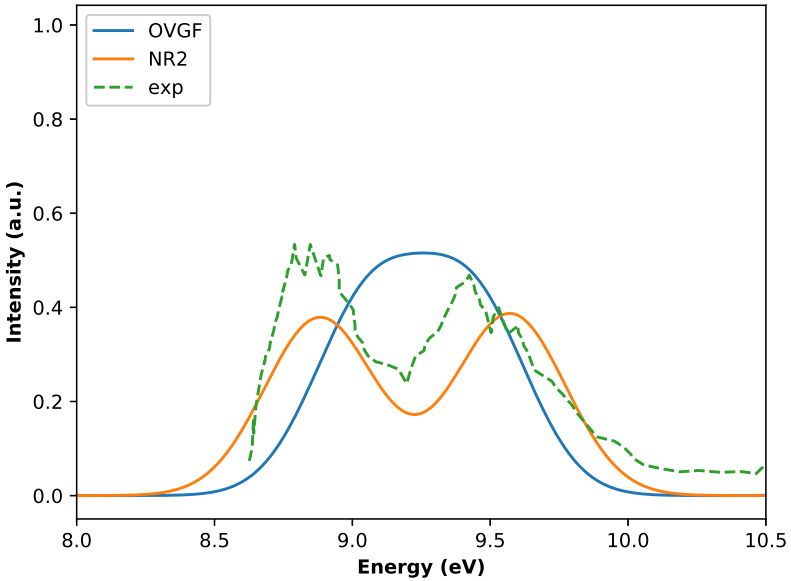

Comparison between calculated and experimental spectra

- Calculated VIEs at NR2 level are closer to experimental results in the outer valence region

---

Experimental data reported in:
R. Gleiter, H. Lange, O. Borzyk, *J. Am. Chem. Soc.*, **1996**, 118, 4889 - 4895.

Computational results published in:
L. Paoloni, M. Fusé, A. Baiardi, V. Barone, *J. Chem. Theory Comput.*, **2020**, 16, 5218-5226.

The case of stella-6-en-2-one

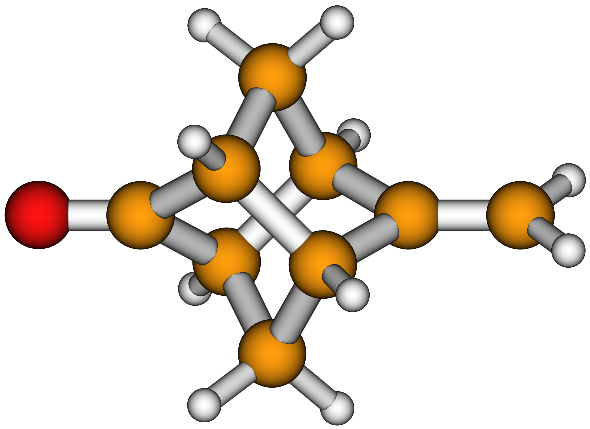

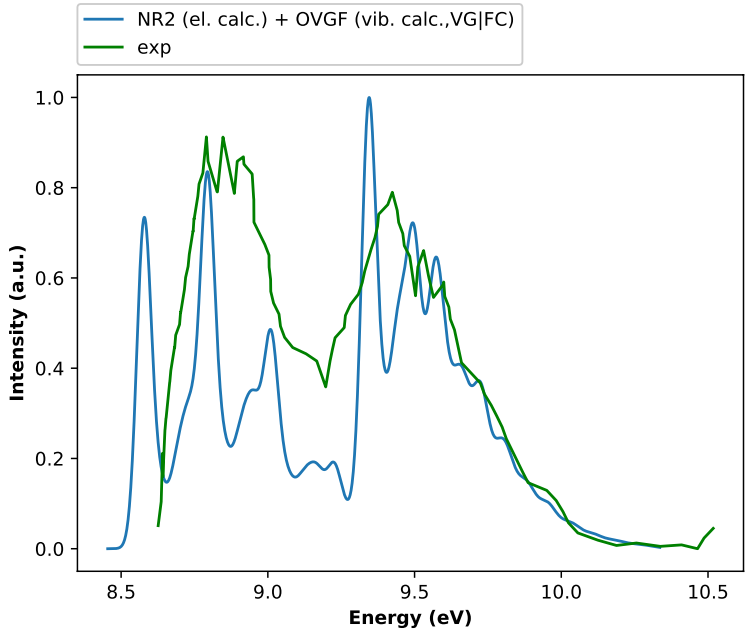

Comparison between calculated and experimental spectra

- Calculated VIEs at NR2 level are closer to experimental results in the outer valence region
- Disagreement between experimental and calculated bandshapes. Why?

Experimental data reported in:
R. Gleiter, H. Lange, O. Borzyk, *J. Am. Chem. Soc.*, **1996**, 118, 4889 - 4895.

Computational results published in:
L. Paoloni, M. Fusé, A. Baiardi, V. Barone, *J. Chem. Theory Comput.*, **2020**, 16, 5218-5226.

Acknowledgements

- Marco Fusé (University of Brescia, Italy)
- Alberto Baiardi (ETH Zürich, Switzerland)
- Vincenzo Barone (Scuola Normale Superiore, Pisa, Italy)
- Paolo Umari (University of Padova, Italy)
- Andrea Sartorel (University of Padova, Italy)

. . . and thanks for your kind attention